iJRASET
International Journal For Research in Applied Science and Engineering Technology

INTERNATIONAL JOURNAL FOR RESEARCH

IN APPLIED SCIENCE & ENGINEERING TECHNOLOGY

Volume: 12 **Issue:** II **Month of publication:** February 2024

DOI: https://doi.org/10.22214/ijraset.2024.58278

www.ijraset.com

Call: 08813907089 | E-mail ID: ijraset@gmail.com

International Journal for Research in Applied Science & Engineering Technology (IJRASET)
ISSN: 2321-9653; IC Value: 45.98; SJ Impact Factor: 7.538
Volume 12 Issue II Feb 2024- Available at www.ijraset.com

Multiscale Deep - CNN Based Target Prediction in Hyperspectral Image with Transfer Learning

Mahaiyo Ningshen[1], Mukesh Kumar Yadav[2], Tarun Nabiyal[3]
Member of Research Staff, Central Research Laboratory, Bharat Electronics Limited

Abstract: ***There are different types of landscape throughout the world which is not readily or directly approachable for human being but their analysis to uncover factual information has become necessary for forming important decision when developing any fresh project. The geographical and landscape scenes can be adequately represented through hyperspectral images captured using remote sensors. The data in the images can potentially be both vast and intricate to analyze and it is essential to consistently perform adequate pre-processing. In this work, we have put up the use of deep learning and transfer learning for object prediction in hyperspectral data. There are mainly two algorithms that have been implemented in this research. The first method is based on Multi-Scale Deep CNN (Convolutional Neural Network) which takes hyperspectral data with varying sizes as the input to detect pixels whose intensity spreads uniformly over many wavelengths or may vary rapidly. Secondly, hyperspectral image sources are not readily available and can be expensive and there are also possibilities for high analysis complexity in the research, so a Transfer Learning based algorithm is applied to the DCNN model. Superior performance in accuracy was noted in the evaluation with respect to the F1 score and recall values for different objects fluctuate between 0.8 to 1.0. Further, we conducted a comparative study, pitting the proposed method against other state-of-the-art target prediction methodologies.***
Keywords: Hyperspectral Imaging, Deep Learning, Convolutional Neural Network, Multiscale Deep CNN, Transfer Learning

I. INTRODUCTION

Remote sensing technology has been an integral element in computer vision research over the years. Remote sensors pos- sess the capability to capture vast expanses of the Earth's geo- graphical area, presenting opportunities for the comprehensive analysis of overall conditions in the given area. Hyperspectral images are composed of a multitude of bands which encom- pass the full spectrum of wavelengths in the electromagnetic spectrum. Henceforth, the data include substantial spectral and spatial details to effectively characterize individual objects. Hy- perspectral data analysis can offer diverse facts about the land- scape suitable for decision making process. The information gathered through the research have been incorporated into nu- merous everyday applications [1]. The traditional methods like RGB (Red, Green, Blue) image processing are not sufficient to process such data. Earth observation data have an extensive number of entities, covering minerals, soils, vegetation, and the like. and manual processing and differentiating such objects is beyond the capacity of the human eye [2][3]. So, an automated mechanism is required for effective processing, feature extrac- tion and object predictions.

Dimensional reduction is one of the key phase in hyperspec- tral data analysis. In hyperspectral data, every pixel is situated at numerous contiguous narrow wavelength bands, and a sig- nificant portion of them exhibit high correlation with each other [4]. Thus, the complexity of analyzing these data is increased unnecessarily when accounting for the overlapping features of various dimensions. De-correlating these bands or features is the main goal of dimensionality reduction, aiding in the separa- tion and processing of valuable bands [5] as indicated in Figure 1. One of the widely adopted techniques for dimensionality re- duction is PCA (Principal Component Analysis), which lever- ages data variance for reduction of the number of wavelength bands within the dataset. However, PCA struggles to efficiently utilize local features due to the low signal-to-noise ratios it en- counters [6]. Thus, the efficiency of hyperspectral data analysis is compromised, leading to a decrease in performance. Tech- niques like regression-based dimensionality reduction, Multidi- mensional Spacing (MDS) and Locality Projection Pursuit (PP) have also been in existence over the years [7][8].

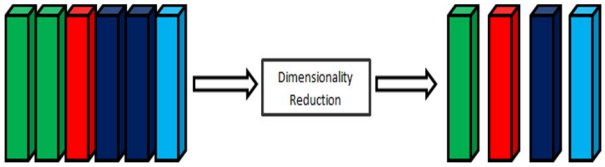

Figure 1: Dimensionality Reduction

Beyond dimensionality reduction, the primary focus of re- search lies in the crucial areas of classification and prediction techniques [9]. Across the years, researchers have devised numerous techniques in these domains. In the early stages of development, methods such as Constrained Signal Detector (CSD), Orthogonal Subspace Projection (OSP), and Adaptive Subspace Detector (ASD) were introduced [10]. With the con- tinuous evolution of neural networks and deep learning, tech- niques based on neural network have also become a promi- nent choice [11]. With its learning and non-linear discrimina- tion ability, it excels in producing highly efficient results. In the realm of supervised techniques, CNN stands out for its ef- fectiveness and high-quality performance. Different manifes- tations of CNN have been developed over time, each with its own merits and drawbacks relative to others[12]. In the fast- paced evolution of modern neural networks, the landscape has witnessed the introduction of more optimized models featuring deeper layers for enhanced learning.

II. RELATED WORK

Target prediction is a binary class classification technique. The prediction process for target pixels involves the utilization of statistical information derived from the background pixels [13]. The performance metrics for these methods are entirely determined by distance measurements. Srivastava et al. [14] introduced an efficient method for differentiating target pix- els from background pixels, leveraging unsupervised transfer learning techniques.

William et al.'s approach [15], which is among the early state-of-the-art prediction techniques, involves the application of the Constrained Energy Minimization (CEM) technique for mapping mine tailings distribution. Other approach like Spec- tral Angle Mapper (SAM) computes the angle difference be- tween the target spectrum and the reference spectrum vectors to assess their similarity. A single target SAM is transition to mul- tiple targets SAM for discriminating tree species based on the reflectance of each species's leaves [16]. Furthermore, Kwon et al. [17] demonstrated the use of a kernel-based, non-linear form of match filter for predicting targets in hyperspectral data. In a comparative study, Tiwari et al.[18] evaluated SAM alongside four prediction algorithms: Spectral Co-Relation Method (SCM), Independent Component Analysis (ICA), Or- thogonal Subspace Projection (OSP) and Constrained Energy Minimization (CEM). Hyperspectral data in real time is known for its high non-linearity and it can introduce difficulties for the linear analysis methods mentioned above, potentially causing a decrease in performance. An Ensemble-based Constrained En- ergy Minimization (ECEM) technique was put forth by Zhao et al. [19] in 2019, aiming to enhance the ability to discrim- inate non-linearity in the data and improve the generalization prowess of the detector. This detector is an extension of the ear- lier CEM model, employing numerous learners for effectively learning and predicting.

As computing technology has advanced in recent years, neu- ral networks have become increasingly crucial in the explo- ration of hyperspectral imagery. Deep Learning (DL) has proven highly advantageous for analyzing data falling in the RGB spectrum, with numerous models applied successfully to achieve optimal performance. On the other hand, hyperspectral image, taken by airborne sensors and satellites, presents pixel values across multiple wavelength ranges, posing numerous challenges for achieving a comprehensive and accurate anal- ysis. Nonetheless, there has been continuous innovation and significant evolution in deep learning has occurred since 2017 [20].

In transitioning from traditional approaches to Deep Learn- ing neural networks, a pivotal change is the adoption of a fully connected architecture, departing from the conventional classi- fier [21]. The models are mathematically structured in a more suitable manner, such as in Recurrent Neural Networks (RNNs) and Convolutional Neural Networks (CNNs). In CNNs [22], layers are designed to perform feature extraction and generate suitable inputs for subsequent stages of analysis. The archi- tectural development began with a uni-dimensional structure, referred to as 1D CNN, and then advanced into 2D and 3D structures. RNNs operate by storing information from previous steps, which is then employed in the processing of subsequent data. RNN demonstrated efficient capability in modeling de- pendencies, whether short-term or long-term within the data's spatial and spectral composition, enabling accurate classifica- tion of hyperspectral imagery [23]. The utility of these models extends to semi-supervised and unsupervised learning scenar- ios.

In his work, Barrera et al.[24] employs a 2D convolutional architecture to effectively discern the internal characteristics of fruits and vegetables using hyperspectral data. It surpasses tra- ditional classifiers, such as SVM. In 2019, Freitas et al. ex- plored a 3D deep CNN for predicting target in maritime surveil- lance [25]. Typically, the availability of hyperspectral im- agery data is constrained, potentially impacting the effective- ness of classification or detection models. Obtaining hyper- spectral data tailored to specific locations or requirements can be prohibitively expensive. To address these challenges, trans- fer learning is employed in deep neural networks, offering a solution to mitigate the limitations imposed [26]. Despite the diverse wavelength ranges at which various hyperspectral data may be captured, there exists common spectral and spatial in- formation among them. Leveraging this shared information, knowledge learned from one dataset can be efficiently applied to predict unknown elements in different data.

This approach not only facilitates effective prediction but also significantly contributes to reducing the computational complexity of the learning model. This study introduces some models and al- gorithms aimed at mitigating the challenges encountered. The proposed methods encompass detection techniques using deep neural networks, as outlined in the research.

III. PROPOSED TARGET PREDICTION MODEL

While all previous CNN models have been designed to ac- cept inputs of fixed sizes, the proposed deep CNN approach has been specifically developed to accommodate variable in- put sizes. This is achieved by configuring various CNN stacks, each tailored to handle different input sizes, yet sharing com- mon parameters, allowing them to operate concurrently. The outputs from the diverse CNN stacks are integrated through a layer, and predictions are subsequently conducted on the con- solidated output. The parallel model here with varied input dimensions proves beneficial in the extraction of extremely low- level features in comparison to other CNN architectures. Subsequently, transfer learning is applied to the CNN, enhancing its ability to leverage the learned features for improved performance. The weights and already trained parameters from a pre- existing model are utilized to train and predict on a different dataset in transfer learning, leading to a significant reduction in the computational overhead of constructing a neural network model with vast amounts of data. The volume of data samples for training is also maximize with transfer learning.

A. Multiscale deep CNN

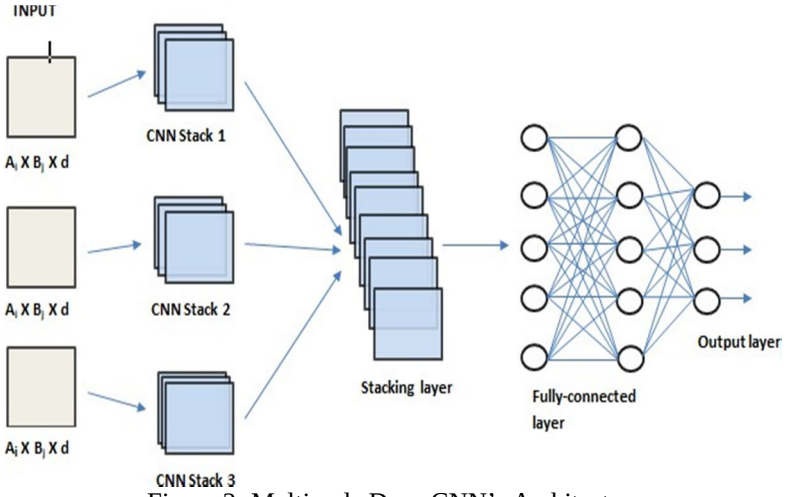

Figure 2: Multiscale Deep CNN's Architecture

Three distinct input sizes are selected and processed through distinct convolutional layers, resulting in the generation of di- verse feature formats for the subsequent prediction process. The features can be represented mathematically as

$$F_i = \sum_{j=0}^{I} x_j \times (A_j \times B_j \times S) \quad (1)$$

where I = Image Size, x = Input,
$A \times B$ = Filters/Kernel Size, S = Number of Wavelength. Pooling is a down sampling operation to reduce the size of the feature input. Here, the maxPool method is used to select the maximum pixel from the pooling area. It is calculated as

$$x_j = max_{i \in Aj}(x_i) \quad (2)$$

where $A_j = j^{th}$ pooling region,
i = index of the pixel in the pooling region
A dense activation layer is added to give non-linearity prop- erties to our model. The output is given as

$$f(x_i) = max(0, x_i) \quad (3)$$

The outputs generated by the three layers are merged within the concatenate or stacking layer, and the combined result is employed for training and predicting of targets.

B. Transfer Learning

The approach is segmented into two stages:

1) Stage 1: Pre-Training

Initially, the proposed CNN undergoes training using a source data. Typically, the source data contains a greater amount of spectral and spatial characteristics compared to our target data. Subsequently, the output and fully connected layers are removed. The result produced from the outstanding layer is employed for subsequent stages. The weights obtained at this point are frozen and will be utilized during fine tuning process. The output feature of the pre-training part is the concatenation of the features obtained using the three convolutional kernels. It is calculated as

$$F_T = concat(F_1, F_2, F_3) \quad (4)$$

where F_1, F_2, F_3 are flattened features obtained using kernel size 3 X 3, 5 X 5 and 7 X 7 respectively

2) Stage 2: Fine Tuning

Fine tuning is performed on our target data leveraging the previously saved model. A fully connected layer is added and training of the data is done only with this layer incorporating the weights of the pre-trained model. The transfer learning model is represented in figure 3.

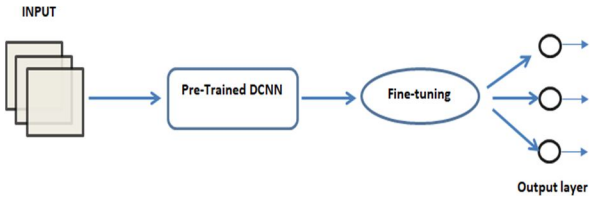

Figure 3: Transfer Learning

The softmax function for predicting the output is calculated as

$$A(y) = \frac{\exp(y_i)}{\sum_{j=1}^{n}\exp(y_j)} \quad (5)$$

where y = Input Vector, $y_i = i^{th}$ Element of the Input Vector
$exp(y_i)$ = Standard Exponential Functions
n = Number of Classes

In general, the model frequently results in extensive training parameters, posing a risk of overfitting. Therefore, L2 regu- larization is incorporated into the dense layer to address this concern.

IV. DATASETS

Three hyperspectral data sets with different pixel composi- tions and different number of wavelength bands used in this research are illustrated in this section. The data is sourced from the Remote Sensing Laboratory, School of Surveying and Geospatial Engineering.

A. Jasper Ridge

The hyperspectral data comprises of 512*614 pixels with 224 bands. Notably, the data is characterized by four primary end members: tree, water, soil, and road. Figure 5 shows the image and ground truth of the data.

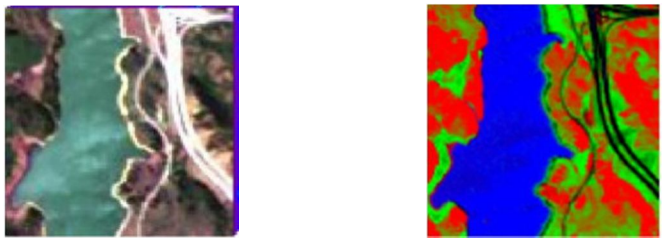

(a) Image (b) Ground Truth

Figure 4: Jasper Ridge Data

B. Indian Pines

It has 145*145 pixels and 224 wavelength bands. There are sixteen objects embedded in the dataset. The image and ground truth is visualised in Figure 4 (a) and (b) respectively.

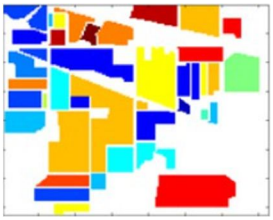
(a) Image


(b) Ground Truth

Figure 5: Indian Pines Data

C. San Diego

The dataset encompasses diverse objects, including buildings, farmlands and runways. Specifically, three aircraft within the dataset are chosen as targets. The data itself is structured with dimensions of 200*200 pixels and comprises 189 spectral bands. The data is visualised in Figures 6(a) and 6(b).


(a) Image


(b) Ground Truth

Figure 6: San Diego Data

V. PERFORMANCE METRICS

We used the following metrics for measuring the perfor- mance of models used in our research.

1) True Positive (TP): It refers to the outcome where a target pixel is accurately identified as a target.
2) False Positive (FP): Here, a background pixel is identified as a target pixel.
3) True Negative (TN): It refers to the outcome where a back- ground pixel is accurately identified as a background.
4) False Negative (FN): Here, a target pixel is identified as a background pixel.
5) Accuracy: It represents the proportion of accurate predic- tions out of the total predictions made by the model. It signifies the overall correctness of the model. It is calcu- lated as

$$Accuracy = \frac{(TP + TN)}{(TP + TN + FP + FN)} \quad (6)$$

6) Precision: It indicates the quality of target detection of the model. It is given by

$$Precision = \frac{TP}{(TP + FP)} \quad (7)$$

7) Recall: It is the percentage of target data that are correctly detected from the total number of target data. It is calcu- lated as

$$Recall = \frac{TP}{(TP + TN)} \quad (8)$$

8) F1 score: It combines precision and recall to give the over- all accuracy of the model.

$$F1score = \frac{(2 * Precision * Recall)}{(Precision + Recall)} \quad (9)$$

9) ROC (Receiver Operating Characteristic) Curve: It is a graphical representation that illustrates the performance of a model at all classification thresholds.

VI. EXPERIMENTAL RESULTS

The methods in our research are implemented using Python 3.11 with TensorFlow and Keras. Additional frameworks, such as Spectral Python, Pysptools, Sklearn, and Numpy, have been used. The results are computed on a Windows operating system equipped with an Intel i5 CPU operating at 2.40 GHz, along with an NVIDIA GeForce 820M graphics card.

A. Multiscale Deep CNN

The multi-scale deep CNN is employed for analysis on the Indian Pines dataset. It has sixteen end members. After im- plementing the de-noising and dimensionality reduction tech- nique, the analysis was carried out using a reduced set of 96 bands. The multi-scale architecture incorporates the three lay- ers of feature extraction, with input sizes of 5*5*96, 7*7*96, and 9*9*96, respectively. Prediction map of multiscale deep CNN is manifested in Figure 7. Table 1 gives the precision, recall and F1 score of every target predicted.

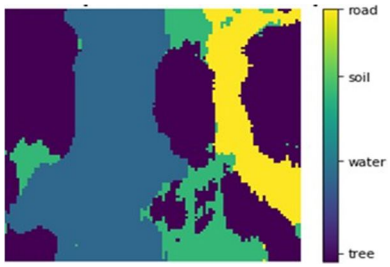

Figure 7: Prediction Map of Multiscale DCNN

Table 1: Performance Report with Multiscale DCNN

	Precision	Recall	F1 score
Tree	.956	.958	.956
Water	.999	.999	.999
soil	.794	.792	.792
Road	.918	.956	.936
			.920

B. Transfer Learning

The model is pre-trained using the Indian Pines dataset as the source data, primarily selected due to its larger sample size with larger composition of spectral and spatial information. Follow- ing the application of noise removal and reduction of dimen- sion, 51 bands are utilized for pre-training stage. In fine tuning, the result from the above pre-training stage serves as the input. A layer for prediction is appended atop the pre-training model for refinement. Then, training of the Jasper Ridge dataset is conducted utilizing the parameters and weights derived from pre-training stage.

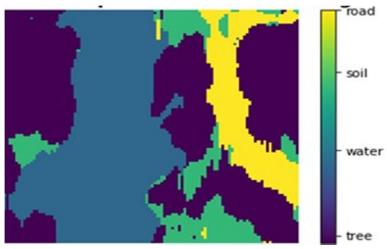

Figure 8: Prediction Map (With transfer learning)

Table 2: Performance Report with transfer learning

	Precision	Recall	F1 score
Tree	.956	.981	.968
Water	.999	.999	.999
soil	.926	.808	.862
Road	.999	.999	.999
			.957

The prediction result using transfer learning is shown in Fig- ure 8. Table 2 gives the performance report. ROC obtained us- ing only multiscale DCNN and with transfer learning is given in Figure 9 (a) and (b) respectively.

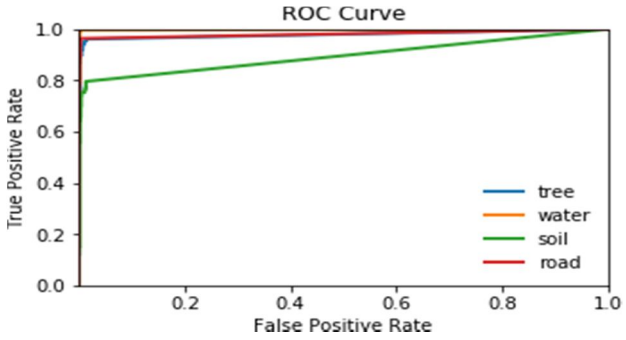

(a)

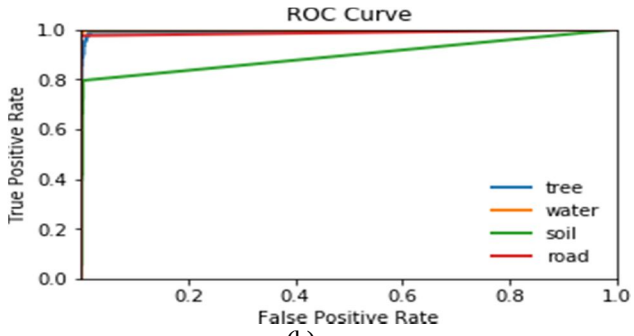

(b)

Figure 9: ROC obtain using a) Multiscale DCNN b) Transfer Learning

In contrast to the multiscale deep CNN, the utilization of transfer learning has resulted in improved precision and recall for individual end members, leading to an overall increase in model accuracy. Apart from this, Transfer Learning also re- duces the training time. In the present experimental setup, the multiscale deep CNN takes approximately 7.83 seconds for one epoch, whereas the transfer learning model completes one epoch in a significantly shorter time, around 1.57 seconds.

C. A Comparative Study Using ECEM and SAM

Two recent approaches, ECEM and SAM are taken for com- parison with our model. ECEM is based on the classical CEM algorithm. Here, a number of CEM detectors are cascaded with sigmoid nonlinear transformation in order to improve the nonlinear discrimination ability of the model. In SAM, a matching process involves calculating the n-dimensional angle between pixels and reference spectra.

The computation of spectral similarity involves treating two spectra as vectors in a space with a dimensionality matching the number of bands and calculating the angle between them. Closer proximity to the reference spectra is indicated by smaller angles. Pixels beyond the designated maximum angle threshold in radians will not undergo classification. The fundamental implementation of both algorithms is executed, and the outcomes are analyzed.

1) Prediction results on Jasper Ridge data using ECEM are shown in figure 10 and the prediction result using SAM is shown in figure 11.

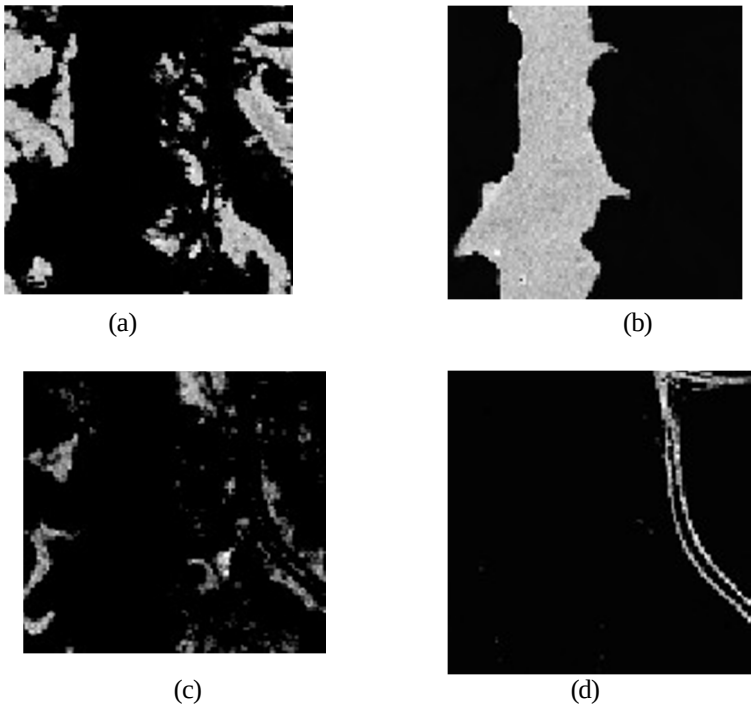

(a) (b) (c) (d)

Figure 10: Predicted Targets (ECEM) a) Tree b) Water c) Soil d) Road

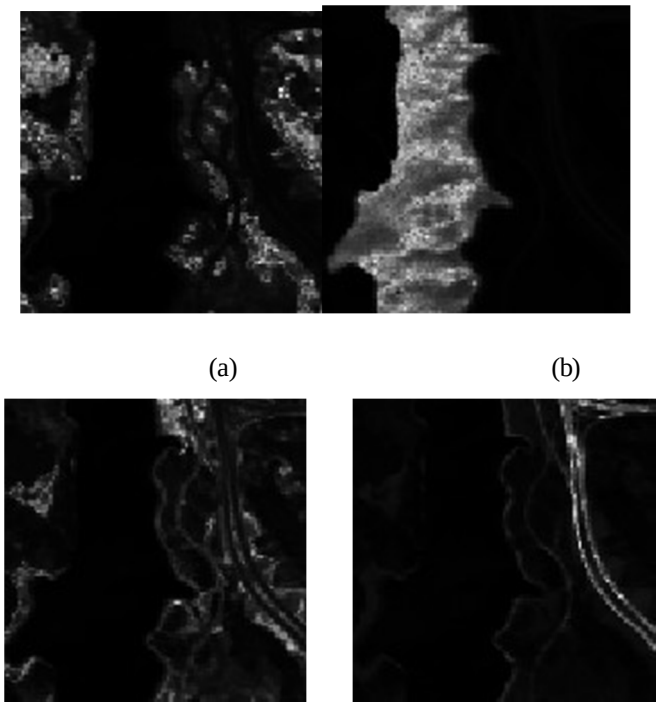

(a) (b) (c) (d)

Figure 11: Predicted Targets (SAM) a) Tree b) Water c) Soil d) Road

Table 3: Performance Comparison of ECEM, SAM and Proposed w.r.t F1 score

Targets	SAM	ECEM	Proposed
Tree	.9949	.9993	.968
Water	.9993	.9992	.999
soil	.5860	.5879	.862
Road	.9982	.9988	.999
	.8946	.8963	.957

Table 3 gives the comparison of the F1 score of predicted targets using SAM, ECEM and proposed method. The result of the above predictions are visualize using the ROC around the F1 score which is given in Figure 12.

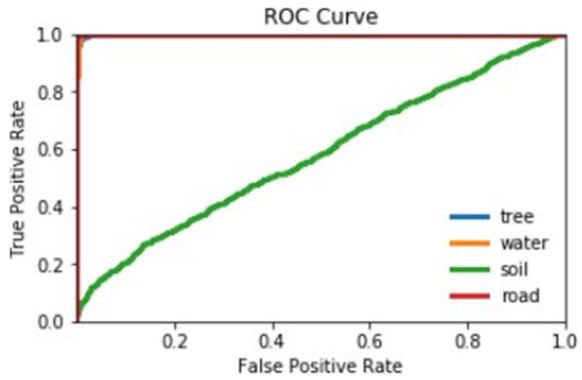

(a)

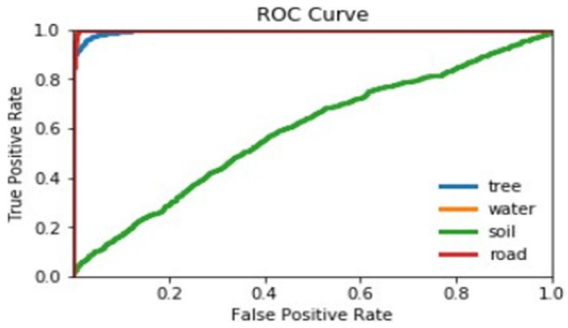

(b)

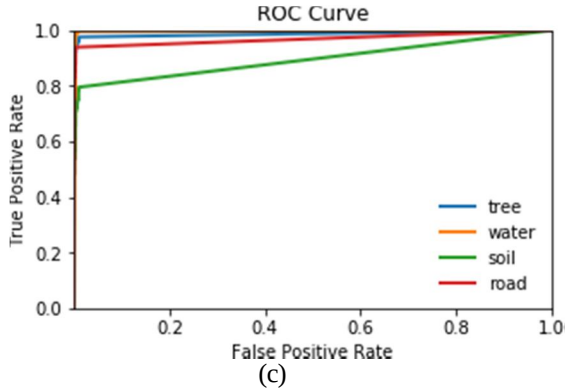

(c)

Figure 12: a) ECEM b) SAM c) Proposed

2) Prediction Results on San Diego Data

Figure 13 represents the prediction result on San Diego data using ECEM, SAM, and our Proposed Model. Table 4 gives the underlying F1 score of the result.

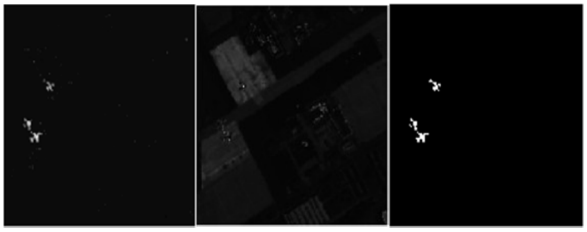

a. (b) (c)

Figure 13: Predicted Results a) ECEM b) SAM c) Proposed

Table 4: Performance Report w.r.t F1 score

	SAM	ECEM	Proposed
Target	.8069	.9995	.9998

In both datasets, the overall performance experienced enhancement through the implementation of our proposed method. In Jasper Ridge, apart from soil, the performance was largely uniform across all targets. This occurrence can be mostly attributed to the original data, where the radiance of the soil's pixels was inherently low, and their resemblance with some other different target. Nevertheless, the accuracy get significantly enhanced by adopting the proposed model. As for San Diego data, ECEM and the proposed method exhibit a similar level of performance. ECEM, as evidenced in pre- vious results, has attained a very high accuracy, focusing pre- dominantly on the detection of single targets. When evaluat- ing both computational efforts and performance, our proposed model demonstrates a distinct superiority in detecting objects within hyperspectral data.

VII. CONCLUSIONS AND FUTURE WORK

The complexity of hyperspectral data, with its multiple layers of information, presents a significant challenge during process- ing and the extraction of specific information. In this study, the prediction of objects has been conducted using hyperspectral data of the Earth's landscape. The application of a multiscale deep CNN classifier on hyperspectral data proved to be more efficient in comparison to existing CNN-based algorithms. Fur- thermore, a transfer learning model was integrated into the mul- tiscale deep CNN. The post-transfer learning performance was evaluated, comparing precision, recall, and F1 score with the original multiscale deep CNN. The results indicated an over- all enhancement in accuracy. Moreover, transfer learning con- tributed to a noteworthy reduction in computational complex- ity. The results obtained from the proposed work were further compared with those of other recent methods for target predic- tion. In subsequent studies, enhancing the robustness of pre- processing and dimensionality reduction can be achieved by de- termining the object type in individual bands using the radiance values. Exploring the use of kernel-based methods may prove beneficial. Additionally, we can configure the transfer learning model to extract insights from multiple data sources through the incorporation of different datasets, thereby enriching features's diversity.

REFERENCES

[1] A. Ozdemir and K. Polat, "Deep learning applications for hyperspectral imaging: A systematic review," Journal of the Institute of Electronics and Computer, vol. 2, no. 1, pp. 39–56, 2020.
[2] P. C. Pandey, K. Manevski, P. K. Srivastava, and G. P. Petropoulos, "The use of hyperspectral earth observation data for land use/cover classifica- tion: Present status, challenges and future outlook," Hyperspectral Re- mote Sensing of Vegetation, 1st ed.; Thenkabail, P., Ed, pp. 147–173, 2018.
[3] A. Vali, S. Comai, and M. Matteucci, "Deep learning for land use and land cover classification based on hyperspectral and multispectral earth observation data: A review," Remote Sensing, vol. 12, no. 15, p. 2495, 2020.
[4] T. Ada˜o, J. Hrus˘ka, L. Pa´dua, et al., "Hyperspectral imaging: A review on uav-based sensors, data processing and applications for agriculture and forestry," Remote sensing, vol. 9, no. 11, p. 1110, 2017.
[5] J. Khodr and R. Younes, "Dimensionality reduction on hyperspectral images: A comparative review based on artificial datas," in 2011 4th international congress on image and signal processing, IEEE, vol. 4, 2011, pp. 1875–1883.
[6] P. Deepa and K. Thilagavathi, "Feature extraction of hyperspectral im- age using principal component analysis and folded-principal compo- nent analysis," in 2015 2nd International Conference on Electronics and Communication Systems (ICECS), IEEE, 2015, pp. 656–660.
[7] V. Laparra, J. Malo, and G. Camps-Valls, "Dimensionality reduction via regression in hyperspectral imagery," IEEE journal of selected topics in signal processing, vol. 9, no. 6, pp. 1026–1036, 2015.

[8] M. Belkin and P. Niyogi, "Laplacian eigenmaps and spectral techniques for embedding and clustering," Advances in neural information process- ing systems, vol. 14, 2001.
[9] C.-I. Chang and S.-S. Chiang, "Anomaly detection and classification for hyperspectral imagery," IEEE transactions on geoscience and remote sensing, vol. 40, no. 6, pp. 1314–1325, 2002.
[10] C.-I. Chang, "Orthogonal subspace projection (osp) revisited: A com- prehensive study and analysis," IEEE transactions on geoscience and remote sensing, vol. 43, no. 3, pp. 502–518, 2005.
[11] S. Hartling, V. Sagan, and M. Maimaitijiang, "Urban tree species clas- sification using uav-based multi-sensor data fusion and machine learn- ing," GIScience &Remote Sensing, vol. 58, no. 8, pp. 1250–1275, 2021.
[12] D. Bhatt, C. Patel, H. Talsania, et al., "Cnn variants for computer vision: History, architecture, application, challenges and future scope," Elec- tronics, vol. 10, no. 20, p. 2470, 2021.
[13] D. Manolakis, E. Truslow, M. Pieper, T. Cooley, and M. Brueggeman, "Detection algorithms in hyperspectral imaging systems: An overview of practical algorithms," IEEE Signal Processing Magazine, vol. 31, no. 1, pp. 24–33, 2013.
[14] N. Srivastava, E. Mansimov, and R. Salakhudinov, "Unsupervised learn- ing of video representations using lstms," in International conference on machine learning, PMLR, 2015, pp. 843–852.
[15] W. H. Farrand and J. C. Harsanyi, "Mapping the distribution of mine tailings in the coeur d'alene river valley, idaho, through the use of a constrained energy minimization technique," Remote Sensing of Envi- ronment, vol. 59, no. 1, pp. 64–76, 1997.
[16] R. H. Yuhas, A. F. Goetz, and J. W. Boardman, "Discrimination among semi-arid landscape endmembers using the spectral angle mapper (sam) algorithm," in JPL, Summaries of the Third Annual JPL Airborne Geo- science Workshop. Volume 1: AVIRIS Workshop, 1992.
[17] H. Kwon and N. M. Nasrabadi, "Kernel spectral matched filter for hy- perspectral imagery," International Journal of Computer Vision, vol. 71, pp. 127–141, 2007.
[18] K. C. Tiwari, M. K. Arora, D. Singh, and D. Yadav, "Military target detection using spectrally modeled algorithms and independent compo- nent analysis," Optical Engineering, vol. 52, no. 2, pp. 026 402–026 402, 2013.
[19] R. Zhao, Z. Shi, Z. Zou, and Z. Zhang, "Ensemble-based cascaded con- strained energy minimization for hyperspectral target detection," Re- mote Sensing, vol. 11, no. 11, p. 1310, 2019.
[20] P. Rajpurkar, J. Irvin, K. Zhu, et al., "Chexnet: Radiologist-level pneu- monia detection on chest x-rays with deep learning," arXiv preprint arXiv:1711.05225, 2017.
[21] J. Xiao, H. Ye, X. He, H. Zhang, F. Wu, and T.-S. Chua, "Attentional factorization machines: Learning the weight of feature interactions via attention networks," arXiv preprint arXiv:1708.04617, 2017.
[22] T.-H. Hsieh and J.-F. Kiang, "Comparison of cnn algorithms on hy- perspectral image classification in agricultural lands," Sensors, vol. 20, no. 6, p. 1734, 2020.
[23] N. Audebert, B. Le Saux, and S. Lefe`vre, "Deep learning for classifica- tion of hyperspectral data: A comparative review," IEEE geoscience and remote sensing magazine, vol. 7, no. 2, pp. 159–173, 2019.
[24] J. Barrera, A. Echavarrıa, C. Madrigal, and J. Herrera-Ramirez, "Clas- sification of hyperspectral images of the interior of fruits and vegetables using a 2d convolutional neuronal network," in Journal of Physics: Con- ference Series, IOP Publishing, vol. 1547, 2020, p. 012 014.
[25] S. Freitas, H. Silva, J. M. Almeida, and E. Silva, "Convolutional neural network target detection in hyperspectral imaging for maritime surveil- lance," International Journal of Advanced Robotic Systems, vol. 16, no. 3, p. 1 729 881 419 842 991, 2019.
[26] Y. Liu, L. Gao, C. Xiao, Y. Qu, K. Zheng, and A. Marinoni, "Hyper- spectral image classification based on a shuffled group convolutional neural network with transfer learning," Remote Sensing, vol. 12, no. 11, p. 1780, 2020.

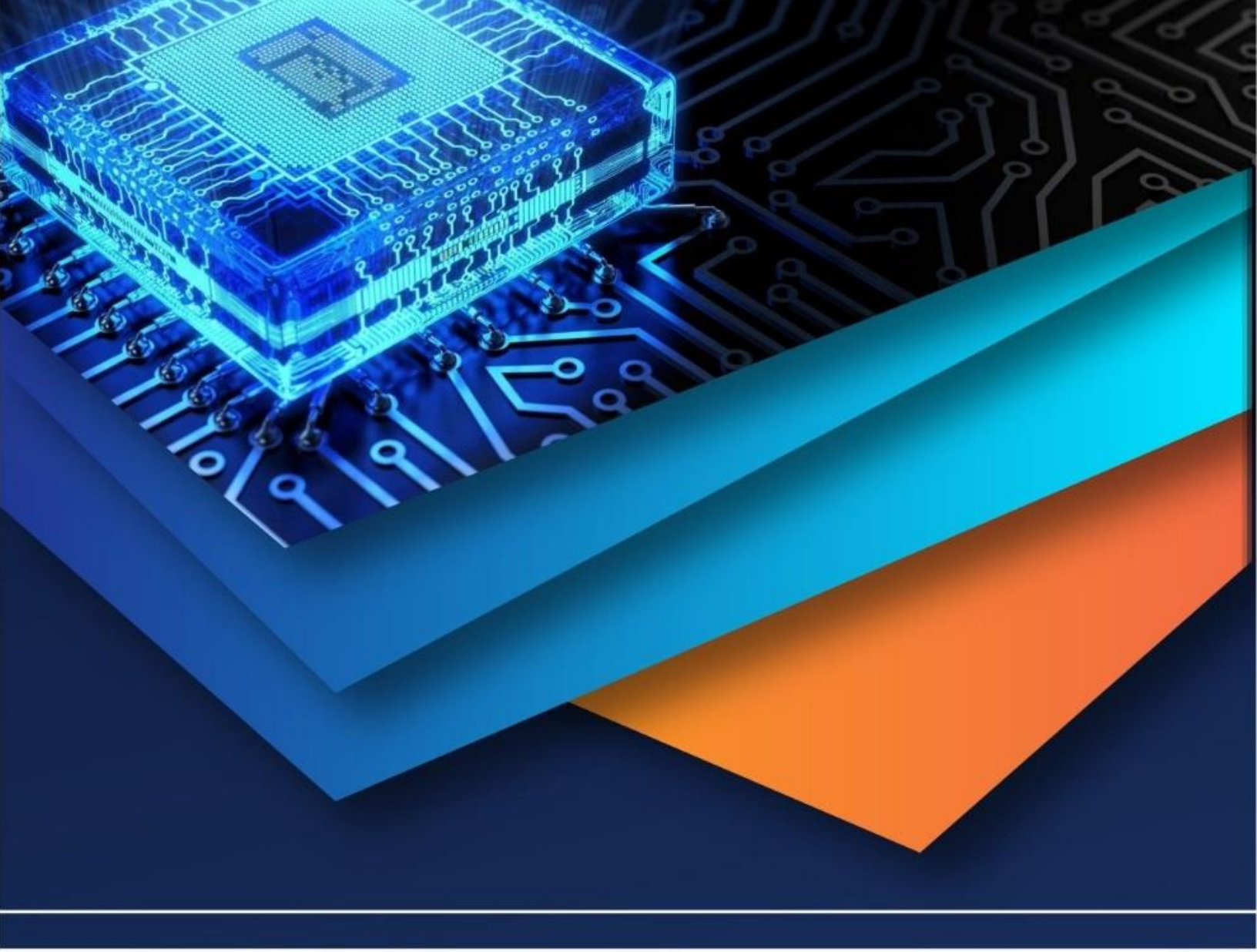

10.22214/IJRASET

45.98

IMPACT FACTOR: 7.129

IMPACT FACTOR: 7.429

INTERNATIONAL JOURNAL FOR RESEARCH

IN APPLIED SCIENCE & ENGINEERING TECHNOLOGY